



室蘭工業大学

学術資源アーカイブ

Muroran Institute of Technology Academic Resources Archive



ハノイ市における繊維質材料混合流動化処理土の埋戻し地盤への適用に関する研究

メタデータ	言語: eng 出版者: 公開日: 2015-12-22 キーワード (Ja): キーワード (En): 作成者: ズウオン, クワン フン メールアドレス: 所属:
URL	https://doi.org/10.15118/00005132

Evaluation on Mitigation of Train-induced Vibration as Using LSS for Backfill Ground of Cut and Cover Tunnel

7.1 INTRODUCTION

As introduced in previous chapters, up to 2020, Hanoi and Ho Chi Minh cities, two huge cities of Vietnam, will have 6 metro lines with more than 100 km in total for each (Luu, 2010). It is forecasted that a huge quantity of excavated soil will be discharged from the construction projects in the two cities over the next decade. Thus, from the environmental point of view, it will become more and more difficult to find reclamation sites for the soil to dump around the cities. Moreover, as operated, the train-induced vibration from the metro lines will be arisen and annoying to nearby resident. This was concluded from the results of the vibration prediction for metro line No.3 in chapter 6, which the vibration level exceeds the threshold of allowable standard, 75 VdB.

Liquefied Stabilized Soil (LSS) used in Japan will be one of the best effective methods to solve the problem of soil generated from tunnel construction sites in Vietnam. However, the researches on application of LSS in metro projects to mitigate train-induced vibration are not found sufficiently in the literatures. Therefore, attempts on research to seek the effect of LSS to characteristics of ground vibration, and then promotion more of using LSS are needed at present.

In this chapter, mitigation of train-induced vibration as using LSS for backfill ground of cut and cover tunnel was evaluated by adopting the numerical analysis procedure established in chapter 6. If the application of LSS can mitigate the ground vibration, it will be a new advantage, and then LSS will be promoted more to use especially in metro projects in Vietnam. Two cases i.e. the use of hill cut soil and LSS as backfilling material

for a cut and cover tunnel section of Hanoi metro line No.3 were selected to analyze in this study. Based on the analysis results, the effect of backfilling materials on mitigation of ground vibration caused by moving train on tunnel was evaluated.

7.2 ANALYSIS PROCEDURES

7.2.1 Simulation of moving train load

In this chapter, the model of train body has been improved, which is modeled as a system of two freedom degrees with consideration of primary and secondary suspension elements. The schematic simplified vertical vibration model of train is shown in Figure 7.1. Like the previous model, the dynamic behavior due to the train-track interaction is typically focused on the effect of periodic or discrete irregularities in the wheel or rail profiles. Thus, the shape function of the irregularities is expressed as following (David, 2005).

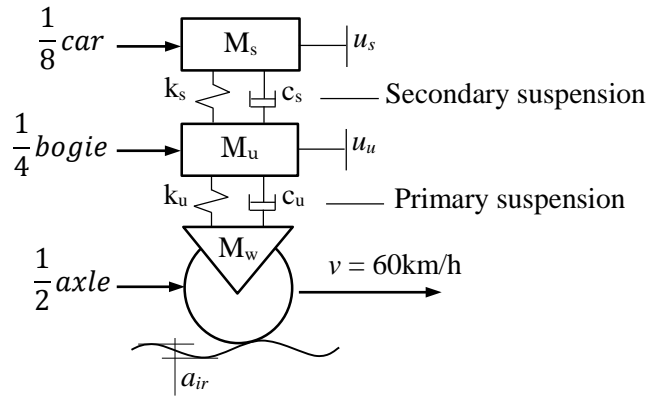


Figure 7.1 Schematic simplified vibration model of train

$$y_{ir}(t) = \sum_{i=1}^3 \frac{a_{ir_i}}{2} \left(1 - \cos \left(2\pi \frac{v}{L_{ir_i}} t \right) \right) \quad (7.1)$$

Where:

a_{ir_i} : i^{th} defect depth (Tore, 2003; David, 2005; Nielsen et al., 2003)

L_{ir_i} : i^{th} wavelength on railhead due to irregularities (Tore, 2003; David, 2005; Nielsen et al., 2003)

v : train velocity

From Figure 7.1, the vertical motion equation of car body was obtained from the model:

$$M_s u_s'' + c_s (u_s' - u_u') + k_s (u_s - u_u) = 0 \quad (7.2)$$

The vertical motion equation of bogie is written as:

$$M_u u_u'' + c_s (u_u' - u_s') + k_s (u_u - u_s) + c_u (u_u' - y_{ir}') + k_u (u_u - y_{ir}) = 0 \quad (7.3)$$

The vertical motion equation of wheel is expressed as:

$$M_w y_{ir}'' + c_u (y_{ir}' - u_u') + k_u (y_{ir} - u_u) + P(t) = 0 \quad (7.4)$$

Be combined (7.2), (7.3) and (7.4), the load applied on wheel is calculated as:

$$P_w(t) = -(M_w y_{ir}'' + M_u u_u'' + M_s u_s'') \quad (7.5)$$

The load applied on rail including static load of train is written as:

$$P(t) = (M_w y_{ir}'' + M_u u_u'' + M_s u_s'') + (M_w + M_u + M_s)g \quad (7.6)$$

To determine $P(t)$, the displacements of u_u and u_s should be determined by solving the second order differential equation set. So this chapter tries to solve the problem by using numerical integral method, Newmark method.

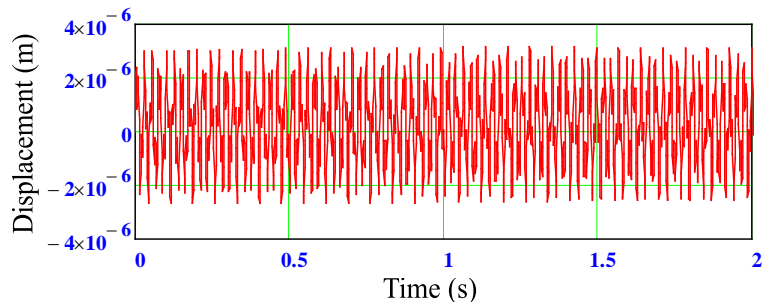
Like the previous model, The $P(t)$ is assumed as a dynamic force on rail and then distributing on tunnel floor through track structure without ballast. Thus, using the theory of infinite Bernoulli-Euler beam supported by elastic foundation with bending stiffness, the general loading function of a moving train is expressed as following.

$$F(z) = \sum_{i=1}^N \sum_{j=1}^n P_{ji}(z) \cdot \Phi_{ji}(z) \quad (7.7)$$

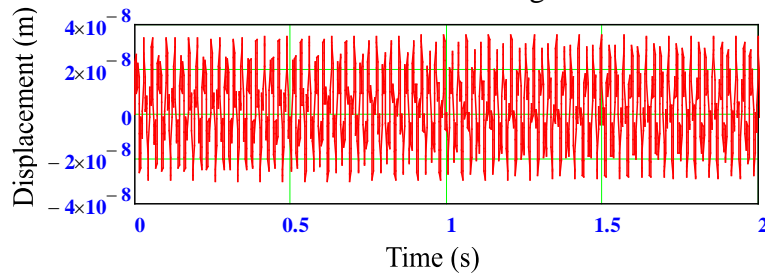
And the moving train load on tunnel floor is written as:

$$F(t) = \sum_{i=1}^N \left[\begin{aligned} &P \left\{ \frac{1}{v} \left(v(t-t_0) - \sum_{j=0}^{i-1} L_j \right) \right\} \cdot \Phi \left\{ v(t-t_0) - \sum_{j=0}^{i-1} L_j \right\} + \\ &P \left\{ \frac{1}{v} \left(v(t-t_0) - \sum_{j=0}^{i-1} L_j - a_i \right) \right\} \cdot \Phi \left\{ v(t-t_0) - \sum_{j=0}^{i-1} L_j - a_i \right\} + \\ &P \left\{ \frac{1}{v} \left(v(t-t_0) - \sum_{j=0}^{i-1} L_j - a_i - b_i \right) \right\} \cdot \Phi \left\{ v(t-t_0) - \sum_{j=0}^{i-1} L_j - a_i - b_i \right\} + \\ &P \left\{ \frac{1}{v} \left(v(t-t_0) - \sum_{j=0}^{i-1} L_j - 2a_i - b_i \right) \right\} \cdot \Phi \left\{ v(t-t_0) - \sum_{j=0}^{i-1} L_j - 2a_i - b_i \right\} \end{aligned} \right] \quad (7.8)$$

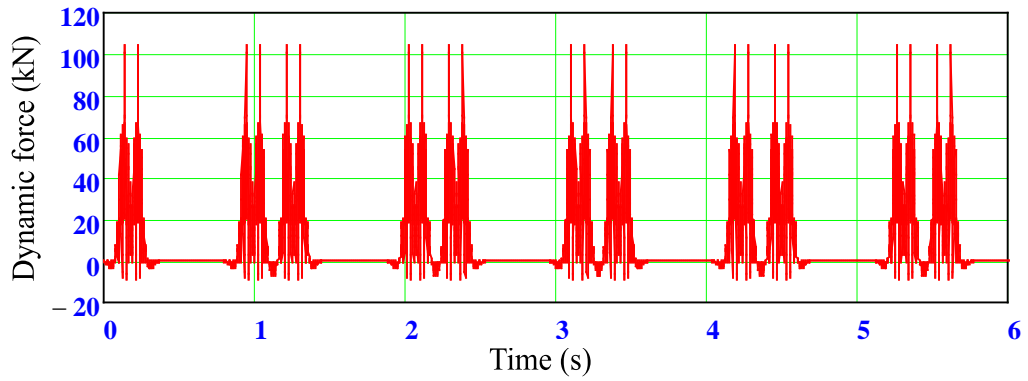
The numerical simulation procedure stated above is accomplished in software Mathcad by programming and detailed in Appendix B with using the calculation parameters of train and track in chapter 6. The numerical results of the dynamic load applied to the tunnel are obtained as shown in Figure 7.2.



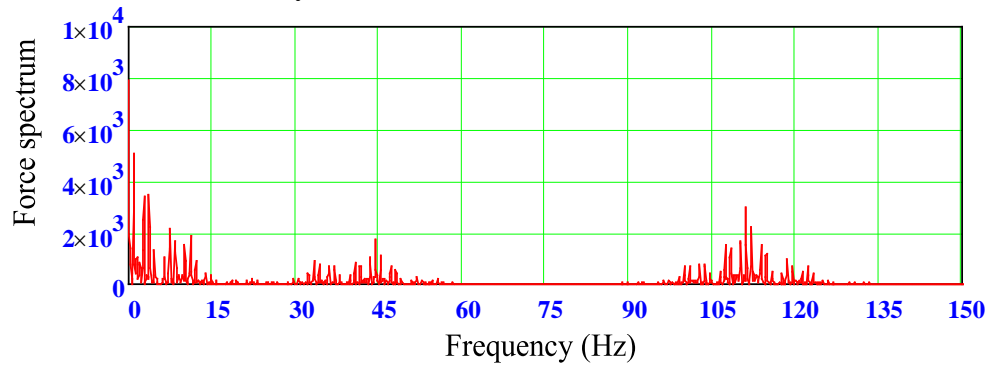
a. Vertical motion of bogie



b. Vertical motion of car body



c. Dynamic load on tunnel from one rail



d. The spectrum of the dynamic force from one rail

Figure 7.2 Characteristic of dynamic load applied to the tunnel

It can be seen from Figure 7.2c and d that the results of dynamic load on train-track system and the spectrum of the dynamic force agree well with that shown in Figure 6.7a and b, respectively. Popp et al. (1999) has commented that in the mid to high frequency range, the dynamic behavior of the car body and the bogies is decoupled by the soft secondary suspension. Moreover, the frequency range of interest for subway induced vibration is 0-80 Hz (Gupta et al., 2007). Thus, a very simple model of the car body is sufficient. Frequently it is even replaced by its constant weight and a kinematic constraint. More detailed models would only be required for ride comfort analysis. Therefore the model established in chapter 6 is reliable to obtain the load time history as input data for Plaxis in solution of the tunnel-soil interaction problem and then prediction of train-induced ground vibration. However, the model made in this chapter can be fundamental one to be improved further for solving more complicated problems regarding to train-railway-track dynamic analysis.

7.2.2 Case study and tunnel, ground conditions

In this study, a cut and cover tunnel section of the metro line No3 in Hanoi city as introduced in previous chapters was selected to analyze. The case study and the ground profile of construction area are schematically shown in Figure 7.3. The tunnel was designed in one-span with width of 10 m and one-story with height of 7 m and backfilled by hill cut soil (case 1) and LSS (case 2) with thickness of 4.5 m, respectively. However, to investigate the effect of the backfilling thickness on the vibration mitigation, case 3 and case 4 was set by burying tunnel deeper and overburdening tunnel by hill cut soil and LSS with thickness of 12m, respectively.

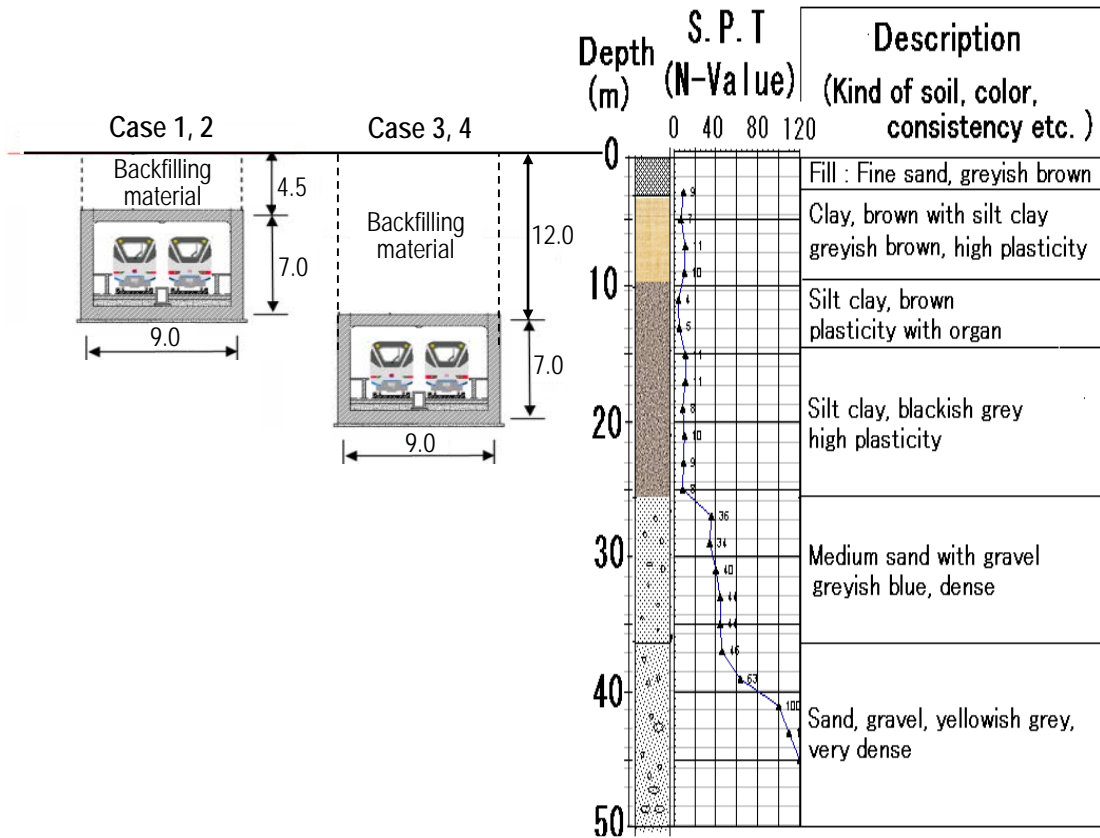


Figure 7.3 Tunnel shape and ground profile

The geotechnical properties of soil layers are shown in Table 7.1. The ground was composed of soft clay and loose sand from the surface to the depth of 30-40 m, and of dense sand or gravel below the depth of 30-40 m. Damping ratio of soil layers is assumed to be 4 %, which in range of 3-8 %, the vibration level of ground is not significantly changed (Das, 1995). Also, most soil types in Hanoi area have the damping ratio in range of 3-5 % (TCXDVN 375, 2006). Poisson's ratio of all soil layers and the backfilling materials were assumed to be 0.49 (Giang, 2010). The shear elastic wave velocity of ground was calculated from N-value, using the formula of Japanese railway standard (Giang, 2010).

Table 7.1 Geotechnical properties of soil layers

Depth (m)	Thickness (m)	Kind	Average N	ν	ρ (kN/m ³)	G (kN/m ²)	V_s (m/s)
2.2	2.2	Sand	9.3	0.49	17.0	48921	168
9.5	7.3	Clay	9.3	0.49	15.0	67447	210
14.1	4.6	Clay	4.5	0.49	15.0	41720	165
25.8	11.7	Clay	9.5	0.49	15.0	68656	212
37.8	12	Sand	40.7	0.49	19.0	146735	275
50	12.2	Sand	98.3	0.49	20.0	278103	369

The parameters of tunnel are shown in Table 7.2. The parameters of train and track were presented in chapter 6. However, in this tunnel section, the velocity of train was designed at speed of 60 km/h. Thus, the numerical simulation procedure of the moving train load for this case is accomplished in Mathcad as detailed in Appendix C.

Table 7.2 Parameters of tunnel

Components	Thickness (m)	ρ (kN/m ³)	Elastic modulus (MN/m ²)	ν
Side wall and ceiling	0.5	25	3500	0.15
Bottom	1	25	3500	0.15
Floor			2500	0.2

7.2.3 Characteristics of backfilling materials

For the present study, the properties of backfilling materials i.e. LSS and hill cut soil used for the analysis model in Plaxis were adopted from the previous research (Giang, 2009), which was estimated in Kohata laboratory, Muroran IT.

Properties of LSS

The original material was Vinhphuc clay taken from a construction site in Hanoi city. The soil is classified into low liquid limit clay (Giang, 2010). The cement stabilizer used was Geoset 10 made by Taiheiyo Cement Co.

Based on results of flow and bleeding tests and unconfined compression tests on samples with 28 days curing, the content of cement stabilizer was assigned to be 200 kg/m³ and the target density of LSS was 1.350 g/cm³.

The deformation coefficient of LSS, $E_0 = 58766$ kN/m² in case of confine pressure of 49 kPa, unit weight, $\rho = 14.0$ kN/m³ and elastic shear modulus, $G = 197200$ kN/m² were set as the basic properties of LSS. The damping ratio of LSS is assumed as 10 % (Giang, 2010).

Properties of hill cut soil

Because there are not much investigation results on stiffness of backfilling material using the hill cut soil, the investigation results on backfilling material in Oohiraki station, which suffered from the Southern Hyogo prefecture earthquake in 1995, were used as the ground constants. N value and unit weight, ρ were set at 10 and 17.0 kN/m³, respectively (Yamata et al., 1996). Elastic shear modulus, $G = 51531$ kN/m² was estimated from N value in accordance with Railway Design Standard (RTRI, 1999). The damping ratio of this material was assumed as 4 %. The physical properties of the two backfilling materials are shown in Table 7.3.

Table 7.3 Physical properties of backfilling material

Backfilling material	V_s (m/s)	ρ (kN/m ³)	h (%)	ν (kN/m ³)
hill cut soil	172	17.0	4	0.49
LSS	370	14.0	10	0.49

7.2.4 Numerical model in Plaxis

Here, a 2D model of tunnel, surrounding soil and dynamic loading of train on tunnel with the use of Plaxis V8 is introduced in order to evaluate the vibrations propagation due to train passage to the ground surface. The modelling procedure in Plaxis was carried out following that as established in chapter 6. However, for the present analysis, the soil behavior is modeled as a linear elastic material. Such a choice is sound by the fact that according to results of numerical modelling in Plaxis 3D for simulating moving loads on typical soil embankment which is designed for high-speed railway trains, both simulation of vertical velocity, which soil was modelled as linear elastic and Mohr-coulomb elastic plastic criterion, respectively show a similar trend in the results (Mojtaba et al., 2014). The geometry of 2D model and element mesh is shown in Figure 7.4 and 7.5, respectively.

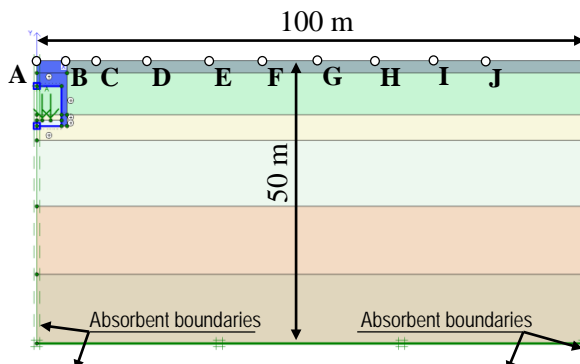


Figure 7.4 View of modelling in Plaxis

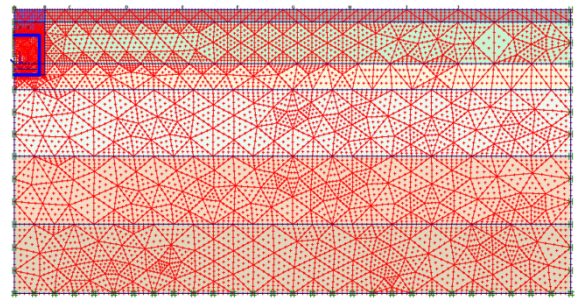


Figure 7.5 Finite element generation in Plaxis

7.3 RESULTS AND DISCUSSION

7.3.1 Vibration velocity in case 1 and case 2

Figure 7.6 to 7.9 show graph of vertical, horizontal and total vibration velocity at points A, B, E and H on ground surface for both cases using the backfilling material of hill cut soil (case 1) and LSS (case 2), respectively. The position of these points is shown in Figure 7.4. By comparing the results for points A~H, it can be observed a decrease in vibration velocity amplitude with distance from tunnel for both cases. As compared at each point, amplitude of the horizontal vibration velocity at A or B in case 2 is significantly lower than that in case 1. One of the most important reasons for this difference in the amplitude between two cases is the stiffness of which LSS is much larger than that of hill cut soil. Thus, the horizontal vibration velocity propagating through LSS from tunnel to ground surface has been damped more than that through hill cut soil. However, amplitude of the vertical vibration velocity at all points in two cases is not considerably different. This is attributed the unit weight of which LSS is not larger than that of hill cut soil. Thus, the vertical vibration velocity is reduced as the tunnel is more overburdened by the backfilling material with larger unit weigh. Therefore, as compared with the hill cut soil, LSS with lower unit weight can hardly reduce the vertical vibration velocity on ground surface, this is interpreted by the results shown later in this study. In addition, with the further points from tunnel such as E or H, the difference in horizontal

velocity amplitude between two cases is narrowed considerably. This is due to the fact that since the LSS is just covered on the top of tunnel, the effect on mitigation of horizontal vibration is essentially observed in nearby range from tunnel center line on ground surface. Thus, the effect is reduced for the further points from tunnel.

Figure 7.10 and 7.11 show the contour of total, horizontal and vertical vibration velocity propagating from exciting point to the ground at the time of 1.5 second after passage of the first car in case 1 and case 2, respectively. The difference in the pattern between two cases can be seen clearly. The dispersion of vibration from exciting point into surrounding soil medium in case 2 tend to be faster than that in case 1. Thus, the vibration in case 2 would be attenuated earlier than that in case 1. The contour of displacement and acceleration for both cases can be seen more in Appendix D.

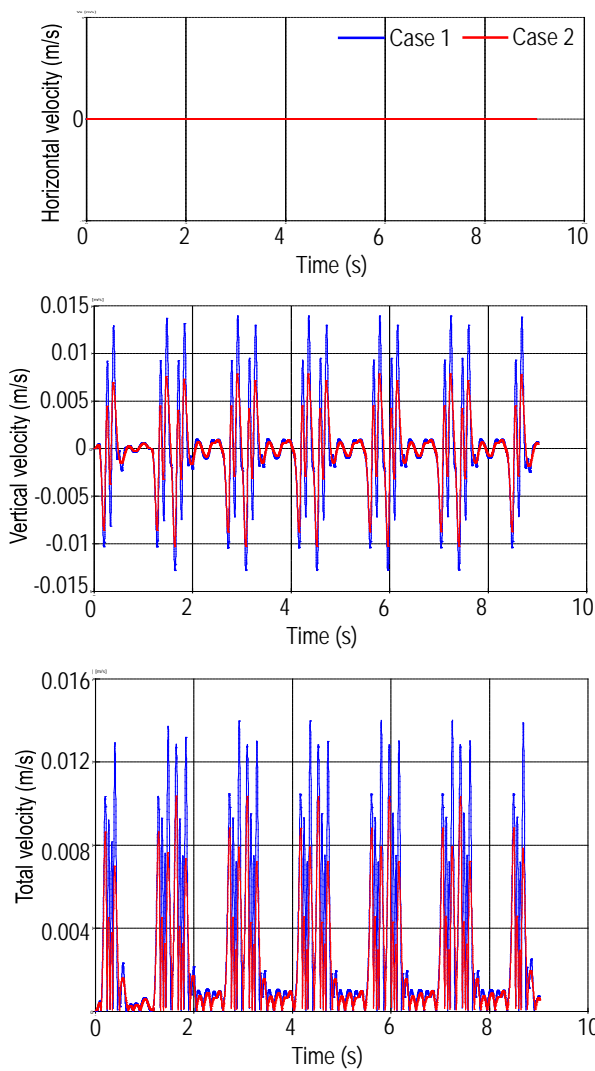


Figure 7.6 Graph of velocity at A in case 1 and case 2, respectively with $v = 60$ km/h

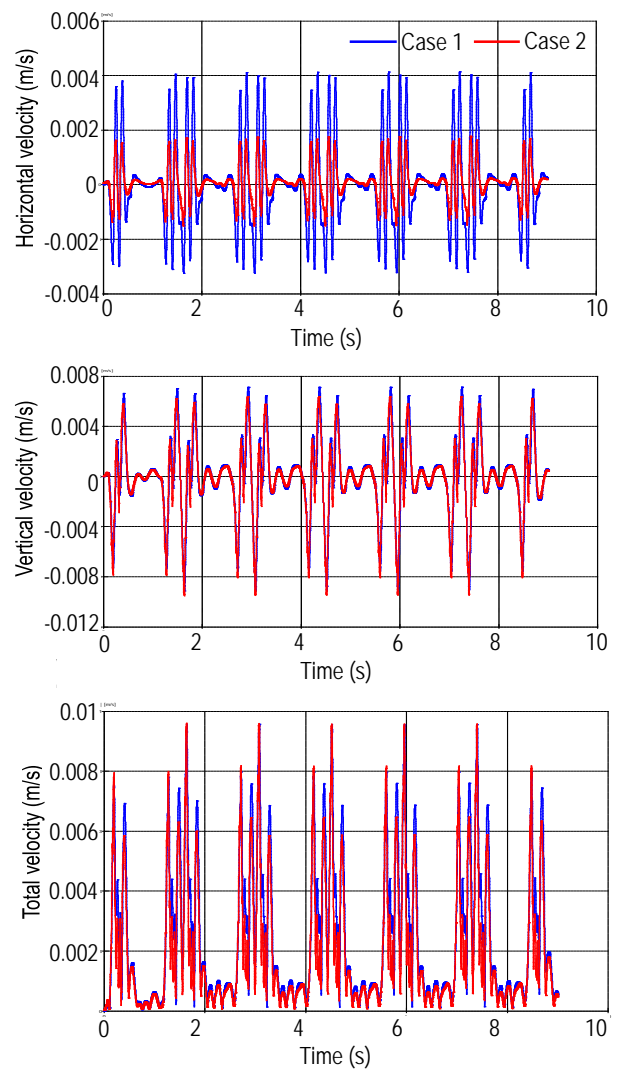


Figure 7.7 Graph of velocity at B in case 1 and case 2, respectively with $v = 60$ km/h

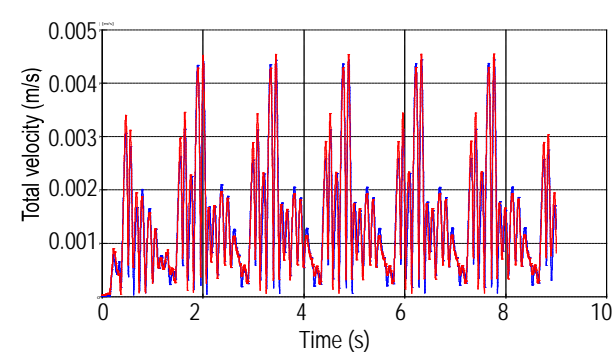
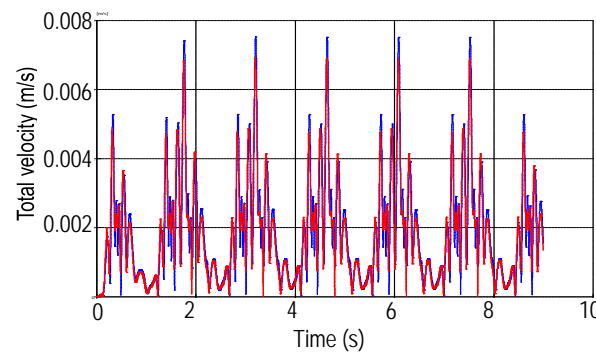
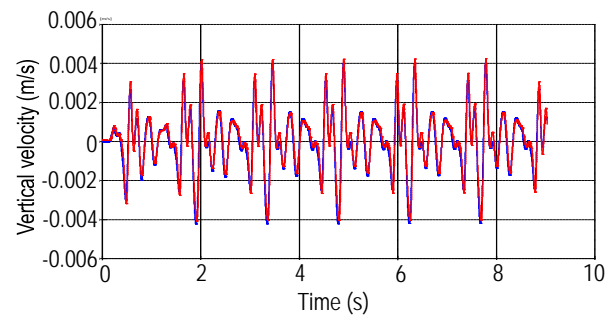
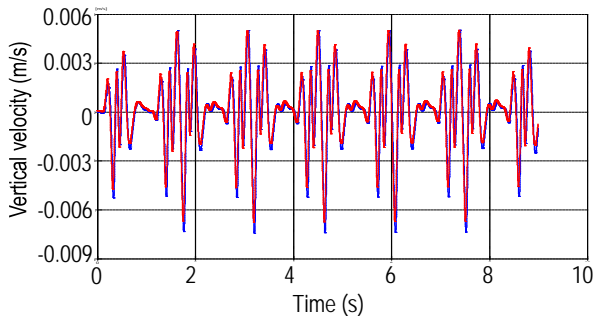
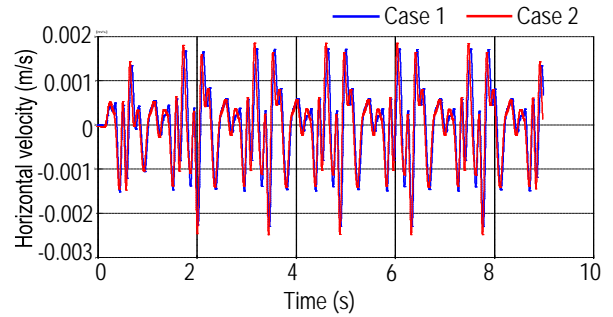
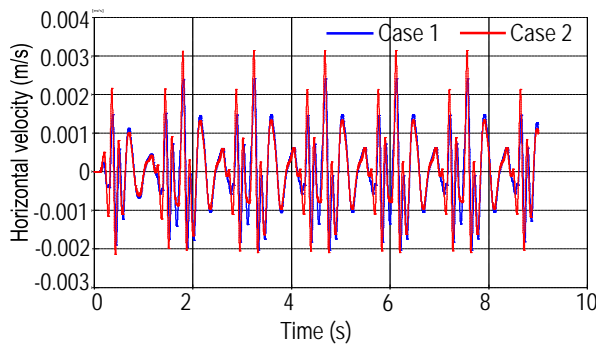


Figure 7.8 Graph of velocity at E in case 1 and case 2, respectively with $v = 60$ km/h

Figure 7.9 Graph of velocity at H in case 1 and case 2, respectively with $v = 60$ km/h

7.3.2 Maximum vibration velocity and level in case 1 and case 2

Figure 7.12 shows relationship between distance and maximum vibration velocity and level for case 1 and case 2, respectively with train velocity of 60 km/h. It can be seen that the level of vibration rapidly decreases with distance away from the tunnel center line for both cases. Moreover, at each point, the level of vibration in case 2 is lower than that in case 1. These differences are due to the difference of backfilling material between two cases. According to the Figure, the effect of LSS on vibration mitigation can be observed apparently. For example, as compared with case 1, the vibration level in case 2 has decreased by 3.29 VdB at point A (zero distance from tunnel center line on ground surface), 1.26 VdB at point B (5.5 m), 0.26 VdB at point E (30 m) and 0.12 VdB at point G (50 m). The nearer points from the tunnel center line on ground surface receive the better effect on the vibration mitigation. The further it is, the more the effect reduces, and the difference in the vibration level between two cases is narrowed. As aforementioned, LSS is just covered on the top of tunnel. Therefore, it has a significant effect on mitigation of vibration for the nearby points from the tunnel on ground surface. In general, subway induced vibration include three basic parts namely source of vibration, route of propagating wave and receiver of vibration. After creation of vibration in the source, these

vibrations propagate into the surrounding medium and then to the receivers (FTA, 2006). Here, the receiver on the ground surface received the vibrations which has propagated through LSS in case 2 would have a lower vibration level than that through the hill cut soil in case 1.

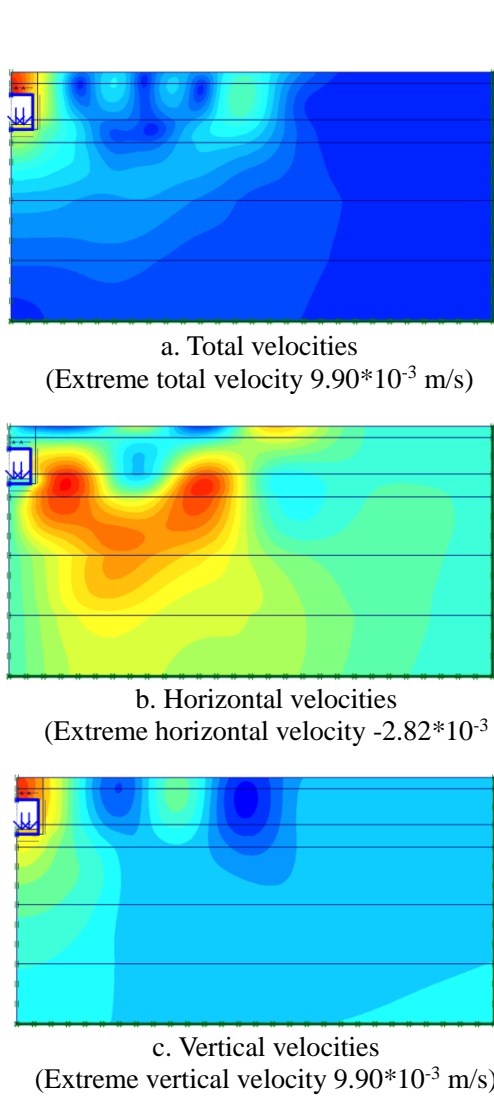


Figure 7.10 Contour of velocity at 1.5 sec of loading in case 1

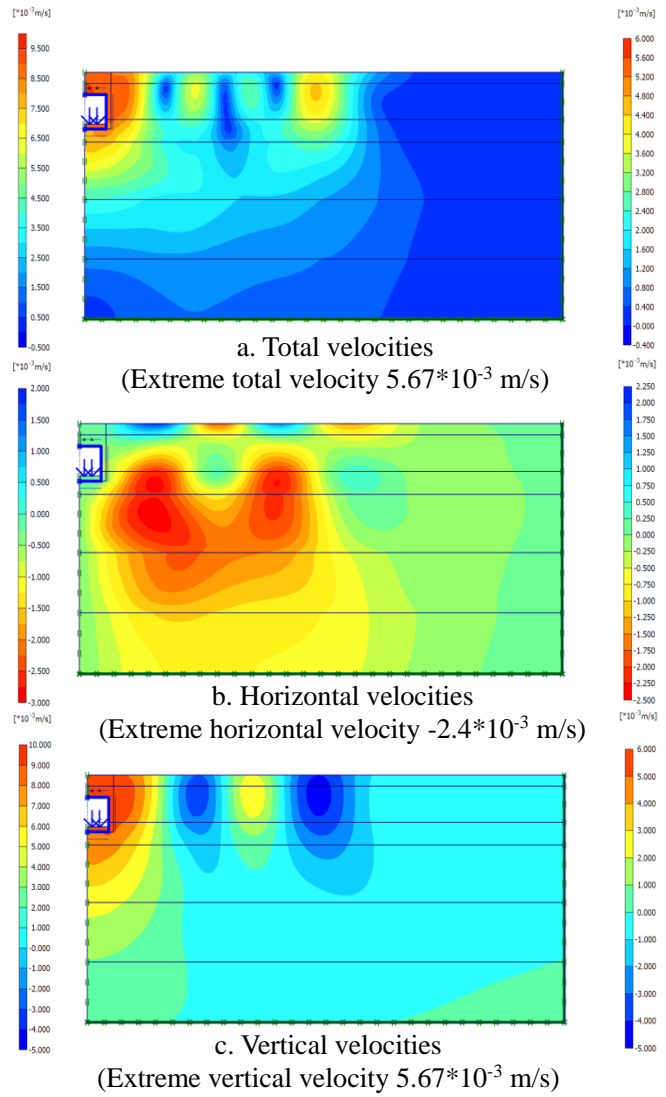


Figure 7.11 Contour of velocity at 1.5 sec of loading in case 2

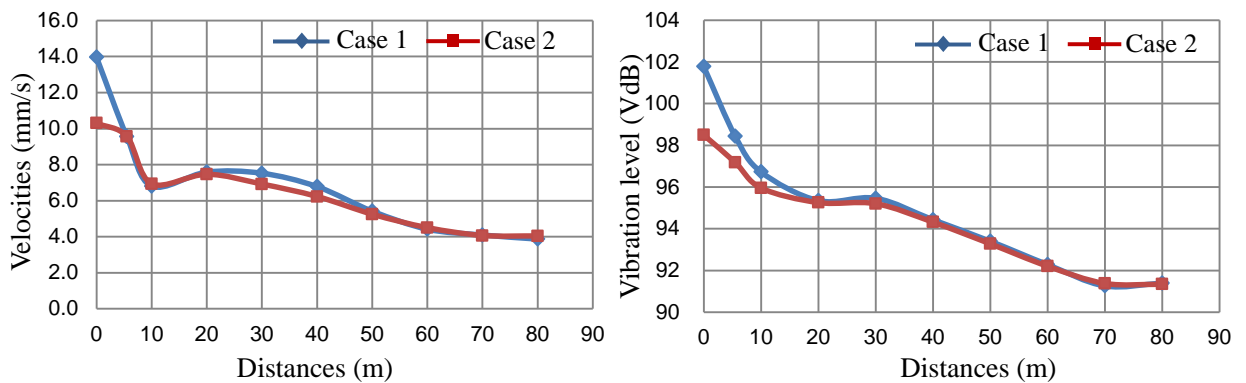


Figure 7.12 Relationship between distance and maximum vibration velocity and level in case 1 and case 2, respectively with $v = 60$ km/h

7.3.3 Vibration velocity in case 3 and case 4

Figure 7.14 shows graph of vertical, horizontal and total vibration velocity at points B on ground surface for both cases using the backfilling material of hill cut soil (case 3) and LSS (case 4), respectively to overburden the tunnel with thickness of 12 m. As compared with results shown in Figure 7.8, it can be seen that the vibration velocity amplitude in case 3 and case 4 is significantly lower than that in case 1 and case 2, respectively. This is due to the fact that the tunnel in two later cases is buried deeper than two previous cases. Thus, the attenuation of vibration with distance results in lower amplitude of vibration in case 3 and 4. Moreover, the horizontal vibration velocity in case 4 is much lower than that in case 3. However the vertical vibration velocity in case 4 tends to be larger. As discussed above, the larger stiffness of backfilling material contributes to reduction of the horizontal vibration velocity on ground surface. Whereas the vertical vibration velocity on ground surface can be lessened as the tunnel is overburdened by backfilling material with larger unit weight. Therefore, the total vibration amplitude at point B in case 4 is not much lower than that in case 3. The similar tendency in results of vibration velocity at other points (A, E, H) can be observed in Figure 7.13, 7.15 and 7.16.

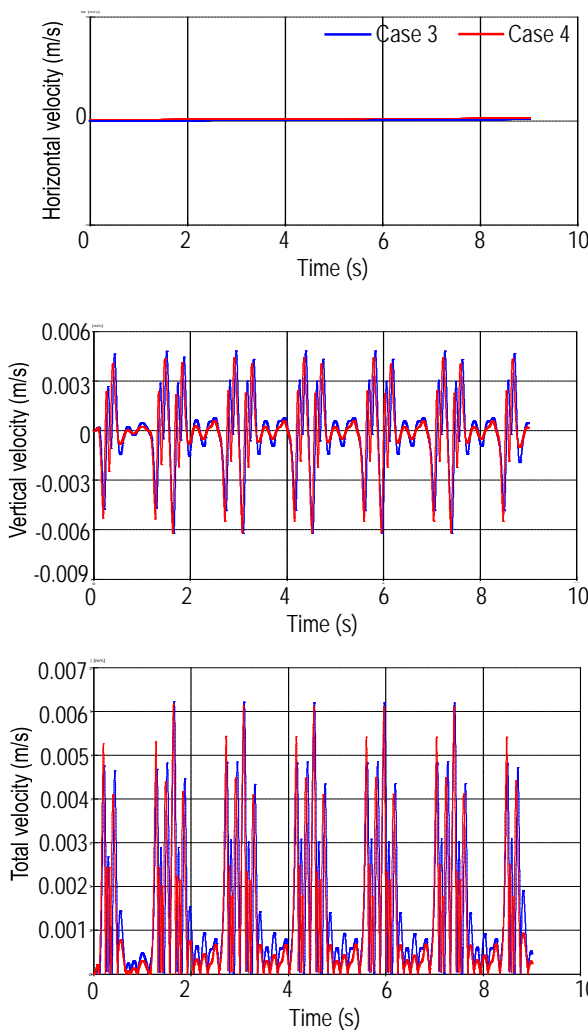


Figure 7.13 Graph of velocity at A in case 3 and case 4, respectively with $v = 60$ km/h

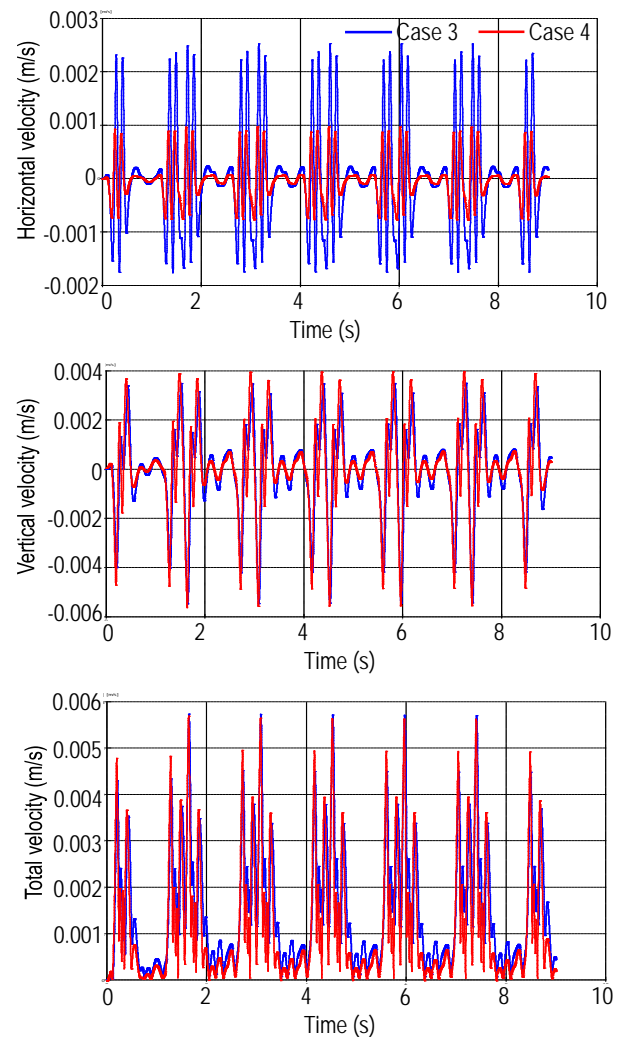


Figure 7.14 Graph of velocity at B in case 3 and case 4, respectively with $v = 60$ km/h

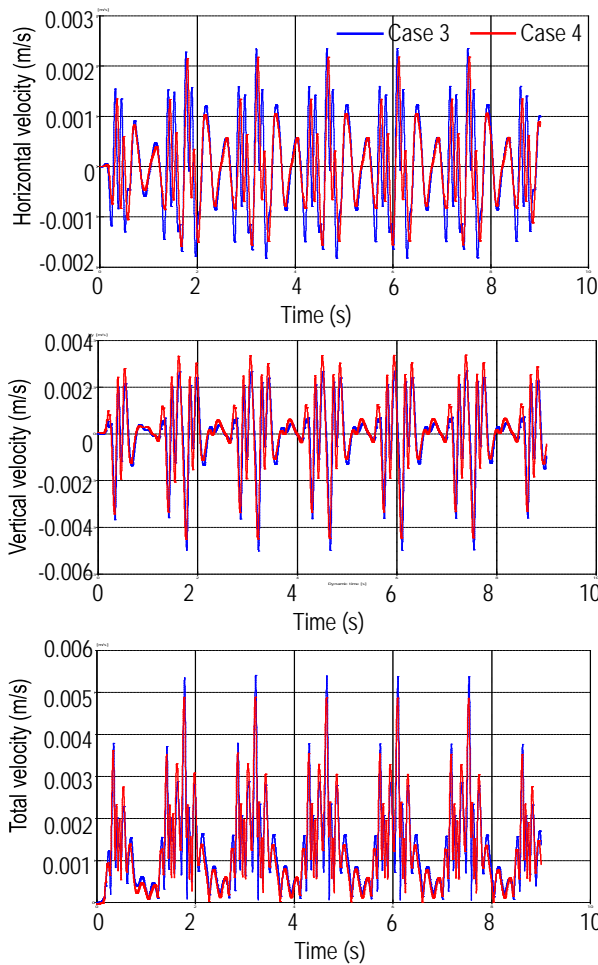


Figure 7.15 Graph of velocity at E in case 3 and case 4, respectively with $v = 60$ km/h

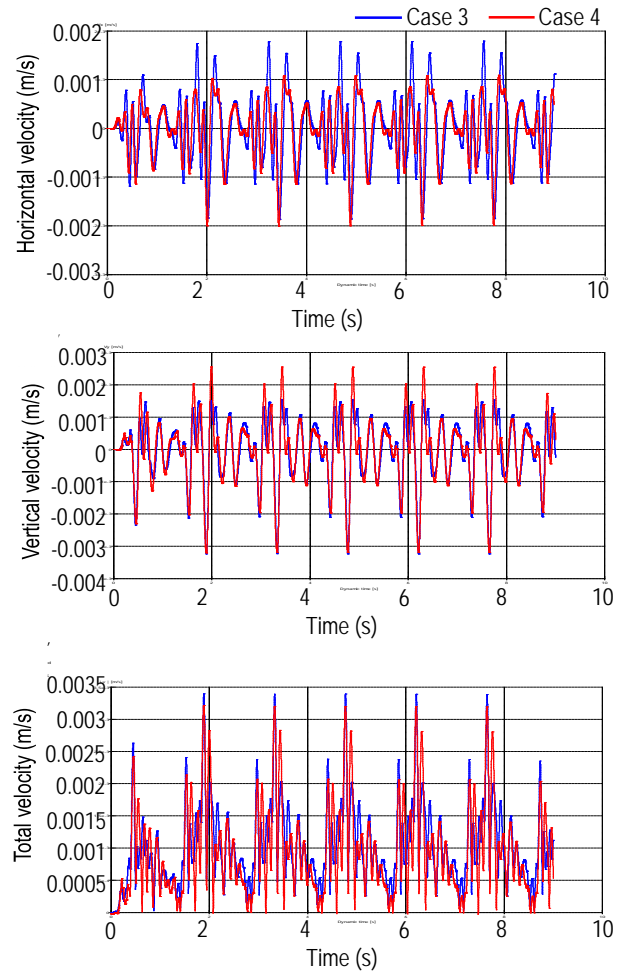


Figure 7.16 Graph of velocity at H in case 3 and case 4, respectively with $v = 60$ km/h

Figure 7.17 and 7.18 show the contour of total, horizontal and vertical vibration velocity propagating from exciting point to the ground at the time of 1.5 second after passage of the first car in case 3 and case 4, respectively. The difference in the pattern between two cases can be seen clearly. Like comparison between case 1 and case 2, The dispersion of vibration from exciting point into surrounding soil medium in case 4 tend to be faster than that in case 3. Thus, the vibration in case 4 would be attenuated earlier than that in case 3. The contour of displacement and acceleration for both cases can be seen more in Appendix E.

7.3.4 Maximum vibration velocity and level in case 3 and case 4

Figure 7.19 shows relationship between distance and maximum vibration velocity and level for case 3 and case 4, respectively with train velocity of 60 km/h. the rapid decreases with distance away from the tunnel center line of the vibration level is also observed for both cases. Moreover, due to deeper distance from the tunnel to ground surface, the level in case 3 and case 4 is much lower than case 1 and case 2, respectively. Also, the effect of LSS on vibration mitigation in case 4 can be observed at nearby positions from the tunnel center line as compared with case 3. For example, the vibration level in case 4 has

decreased by 0.67 VdB at point A (zero distance from tunnel center line on ground surface), 0.08 VdB at point B (5.5m) and 0.82 VdB at point C (10m). From D (20 m) and further, the level in case 4 is slightly larger than that in case 3. As discussed above, though the larger stiffness of LSS in comparison with hill cut soil contributes significantly on mitigation of the horizontal vibration velocity on the ground surface, its lower unit weight cannot reduce the vertical vibration velocity. Because of the fact that the vibration on the ground surface is reduced as the tunnel is more overburdened. Therefore, the deeper the tunnel is buried, the more the effect of LSS against the hill cut soil on vibration mitigation reduces. It means that reduction of vibration level on ground surface by using LSS is less than that by using hill cut soil as the tunnel is buried deeper. For example, as changing the depth of tunnel from case 1 to case 3, the level has decreased by 7.29 VdB at A, 3.1 VdB at D and 3.3 VdB at H. Meanwhile, from case 2 to case 4, the level has decreased 4.68 at A, 2.91 VdB at D and 3.03 VdB at H. However the level at the nearby points in case 4 is lower than that in case 3. Thus, it is considered that LSS has an effective potential in mitigation of vibration, especially at the nearby position which is strongest impacted from the train-induced vibration.

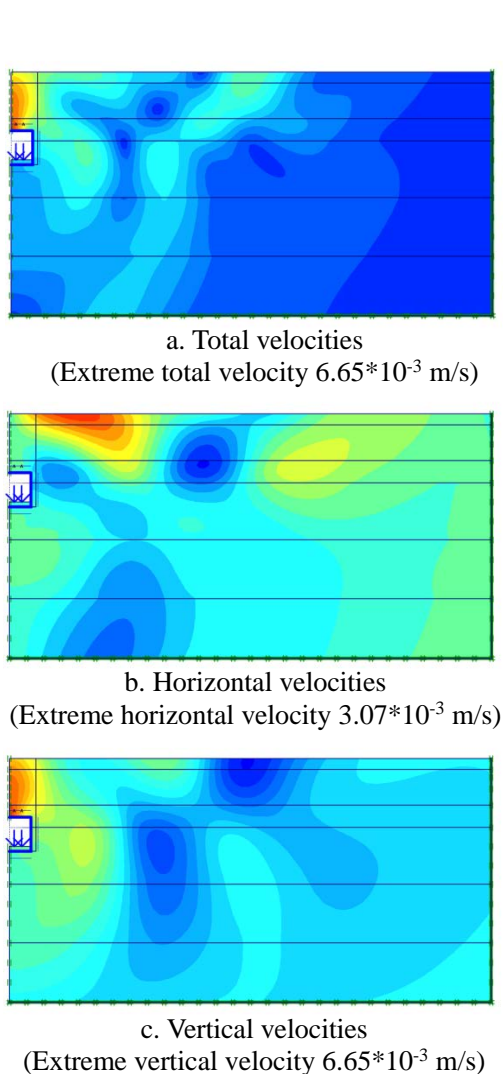


Figure 7.17 Contour of velocity at 1.5 sec of loading in case 3

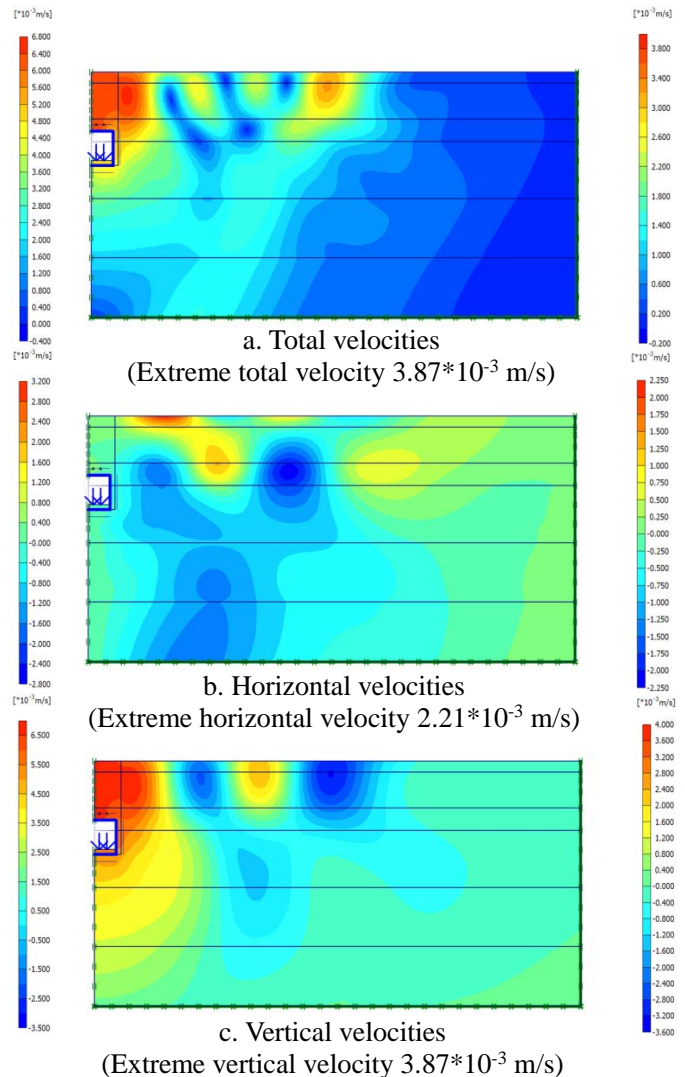


Figure 7.18 Contour of velocity at 1.5 sec of loading case 4

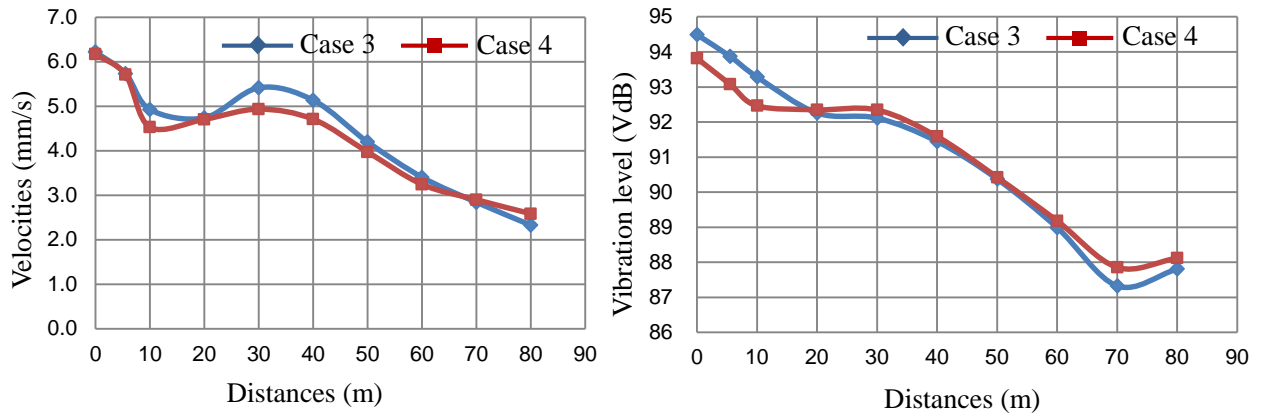


Figure 7.19 Relationship between distance and maximum vibration velocity and level in case 3 and case 4, respectively with $v = 60$ km/h

7.4 SUMMARY

Focused on the utilization of general hill cut soil and LSS as backfilling material, the effect of ground vibration mitigation was studied for cut and cover tunnel of metro line No3 in Hanoi city. In this chapter, the ground vibration properties were studied analytically using the numerical procedure established in previous chapter. The model of train body has been improved which is modeled as a system of two freedom degrees with consideration of primary and secondary suspension elements. The result of the model in term of the load time history can be input data for numerical model in solution of the tunnel-soil interaction problem and then prediction of train-induced ground vibration. Based on the analysis results, the conclusions were withdrawn as following.

As compared with hill cut soil, LSS had the significantly better effect on mitigation of ground vibration induced by moving train in the cut and cover tunnel section of metro line No3 in Hanoi city due to its larger stiffness, especially at nearby position from the tunnel center line on the ground surface. At further position, the effect was reduced because of the fact that LSS is just covered on the top of the tunnel.

In case of assumption which the tunnel was buried deeper, the analysis results indicated that effect of LSS on mitigation of vibration has been reduced in comparison with hill cut soil. This is attributed the unit weight of which LSS is not larger than that of hill cut soil. However, the level at the nearby points from the tunnel center line on the ground surface which is strongest impacted from the train-induced vibration in case of using LSS is lower than that of using hill cut soil.

From the above, it was concluded that LSS had an effective potential as countermeasure against train-induced vibration in cut and cover tunnel. This property was pointed out as a new advantage of LSS.

Based on the numerical results in this chapter and other in previous chapters, it is considered that one of the most important parameters of backfill material which influences on mitigation of train-induced vibration is the stiffness of the material. Therefore, it is predicted that LSS mixed with the crushed newspaper as a fiber material

with its larger stiffness than that of the pure LSS will be more effective on mitigation the vibration. This will be performed in the coming time.

Moreover, it is suggested that LSS mixed with the fiber material in this study can be used as aseismatic material which is exposed to dynamic loading such as traffic loading, earthquake loading usually occurs in Japan, though more research works for this need to be carried out in the coming time.

REFERENCES

Luu, D. H. (2010): Metro-a mode of indispensable public transportation in big cities, *Journal of Vietnam federation of civil engineering association* (in Vietnamese).

David, M. S. (2005): Identification and development of a model of railway track dynamic behavior, *a thesis submitted for the degree of master of Engineering – Queensland University of Technology*.

Tore, D. (2003): Railway track dynamic - a survey, *solid mechanics/IKP*, Linköping university, Sweden.

Nielsen, J. C. O., Lunden, R., Johansson, A. and Vernersson, T. (2003): Train-track interaction and mechanisms of irregular wear on wheel and rail surface, *Vehicle system dynamics*, Vol.40, issue 1-3, pp.3-54.

Popp, K., Kruse, H. and Kaiser, I. (1999): Vehicle-track dynamics in the mid-frequency range, *Vehicle System Dynamic*, Vol. 31, No.5-6. Pp.423-464

Gupta, S., Hussein, M. F. M., Degrande, G., Hunt, H. E. M. and Clouteau, D. (2007): A comparison of two numerical models for the prediction of vibrations from underground railway traffic, *Soil and dynamic and earthquake Eng.*, 27, pp.608-624

Giang, N. C. (2010): Study on advanced effective utilization of excavated soil in Hanoi city – Vietnam, *a thesis, division of civil and environmental engineering; graduate school of Muroran Institute of technology*.

TCXDVN (2006): Design of structure for earthquake resistance, construction standard of Vietnam, *p.1, regulations, earthquake impact with building structure* (in Vietnamese)

Railway Technical Research Institute (1999): Explanation for railway structure and design standards.

Das, B. M. (1995): Principles of soil dynamic, PWS-KENT, *publishing company, USA*.

Mojtaba, S., Mohamad, R. S. S., Karl, J. W., Thomas, M. (2014): 3D modelling of train induced moving loads on an embankment, *Plaxis bulletin, Autumn issue 2014, www.plaxis.com*, pp.10-15.

FTA (2006): Transit noise and vibration impact assessment, *Office of planning and environment – Federal Transit Administration*.